RESEARCH ARTICLE

Optimization of nitrate removal from aqueous solutions using clinoptilolite /$CoFe_2O_4$ by surface response methodology

A. Houshangi[1], M. Yousefi[2,*], S. Jamebozorgi[3], R. Ghiasi[4]

[1] Department of Chemistry, Faculty of science, Arak Branch, Islamic Azad University Arak, Iran

[2] Department of Chemistry ,Yadegar-e Imam Khomeini(RAH) Shahr-e Rey Branch, Islamic Azad University, Tehran, Iran

[3] Department of Chemistry, Faculty of science, Hamedan Branch, Islamic Azad University Hamedan, Iran

[4] Department of Chemistry, Faculty of science, East Tehran Branch, Islamic Azad University Tehran, Iran

ARTICLE INFO

Article History:
Received 2020-05-20
Accepted 2020-07-11
Published 2020-08-01

Keywords:
clinoptilolite
clinoptilolite /$CoFe_2O_4$
removal
nitrate
RSM

ABSTRACT

The purpose of this study was to investigate the efficiency of clinoptilolite modified with magnetic $CoFe_2O_4$nanoparticles as an adsorbent in the removal of nitrate from aqueous solutions. Clinoptilolite and clinoptilolite/ $CoFe_2O_4$werecharacterized by X-ray diffraction (XRD), Fourier-transform infrared spectroscopy (FTIR), scanning electron microscopy (SEM), Transmission electron microscopy (TEM), Brunauer-Emmett-Teller (BET) analysis and Barrett-Joyner-Halenda (BJH), and vibrating sample magnetometer (VSM) techniques. The average particle size calculated by the Debye–Scherrer for clinoptilolite and clinoptilolite/$CoFe_2O_4$ were about 31 nm and 42 nm, respectively.Based on the (SEM) results,the average particle size was comparable with the Debye Scherrer calculated crystallite size. BET shows that the surface area increased from 18.42 to 25.95 m2 g^{-1} by the modified clinoptilolite surface. The clinoptilolite/$CoFe_2O_4$ has saturation magnetization 0.97 emu/g.Thenitrate adsorption capacity was evaluated by clinoptilolite and clinoptilolite/$CoFe_2O_4$.Based on the results, the adsorption capacity of the clinoptilolite/$CoFe_2O_4$had a higher adsorption capacity than the unmodified clinoptilolitewhich can be attributed to its higher surface area. The effect of different variables on the nitrate removal process, such as temperature, time and mass of adsorbent, was optimized using the surface response methodology (RSM) with the Box-Behnken(BBD) method. The study showed that the maximum removal percentage of nitrate was 97.03% at 55 °C, 40.36 h, and 0.27 g mass of adsorbent.

How to cite this article
HoushangiA., Yousefi M., Jamebozorgi S., Ghiasi R. Optimization of nitrate removal from aqueous solutions using clinoptilolite /CoFe2O4 by surface response methodology. J. Nanoanalysis., 2020; 7(3): 166-178. DOI: 10.22034/jna.001.

INTRODUCTION

Nitrate is one of the mineral anions that results from elemental nitrogen oxidation. It is an essential element for protein synthesis in plants and plays an important role in the nitrogen cycle. Concerns about nitrate levels around the world have been due to the decline in the quality of surface water and underground water over the past four decades [1-5].Among the sources of pollution of groundwater to nitrates, wastewater, sewage, and animal waste can be mentioned. Its complications include methemoglobinemia, infant mortality, carcinogenic nitrosamine production in adults, the probability of an abortion outbreak and other diseases. Also, nitrate can cause water resources and problems associated with it. The World Health Organization sets the standard level of 50 mg/L of nitrate concentration in regularly used drinking water where nitrate is soluble and stable in water [6]. Conventional water purification methods, including chlorination [7],coagulation [8],and filtration are

* Corresponding Author Email: *Email*

not suitable for the removal of this material and therefore, advanced refining methods are required to include ion exchange [9], electrodialysis[10], electrochemical [11],etc. Among the limitations of the physicochemical treatment systems are the high cost of utilization and the problem of sewage disposal. Even more seriously, in some cases side products are produced that are more dangerous than the primary pollutant. The problems of biological methods include limited supply of organic substrate, sludge production and high care needs. On the other hand, due to the advantages of the adsorption method such as cheapness, rapid adsorption, high adsorption capacity, resilience and reuse, this method is very important [12]. Over the past years, more than 50 types of natural zeolite have been identified, the most important of which includeanalcime, chabazite, and clinoptilolite [13]. Natural clinoptilolites have widely been used for metal removal from industrial wastewaters due to their chemical resistance and low cost, even if their exchange capacity for heavy metals is about 30% of the total capacity. Clinoptilolite is a low-cost, accessibility, and usable adsorbent on an industrial scale.Zeolites have a three-dimensional aluminosilicate structure. For all four faces of AlO_4 in the zeolite network, a negative charge is generated on the network. Silicon is in the form of cation Si^{4+} and aluminum as Al^{3+} cation. The negative loads generated by the cations in the network are neutralized. The network has canals or holes connected to each other, which are occupied by water and cations. These cations have mobile networks and, due to this mobility, provide the cation exchange effect for zeolite. In other words, zeolites are hydrated aluminosilicate crystals that contain cations of alkaline and alkaline metals, and have unlimited structures [14].The properties of these compounds can be cation exchangers, and have the ability to reverse the adsorption and discharges of water without causing a major change in their molecular structure. Since the surface of zeolites has a negative charge, zeolite should change the surface charge potential of zeolite to remove the anions by zeolite.The surface correction of zeolites is done by materials such as surfactants and other materials such as iron oxide, which can change the surface of zeolites and convert zeolites into an ionic replacement material. The correction of zeolite surfaces by cobalt ferrite nanoparticles enhances its efficiency[15-25].The magnetic MWCNTs with adsorbed analytes were easily separated from the aqueous solution by applying an external magnetic field [26]. A magnetic graphitic carbon nitride as a new adsorbent for simple separation of Ni (II) ion from foodstuff by ultrasound-assisted magnetic dispersive micro solid-phase extraction method [27]. Separation and determination of lead in human urine and water samples based on thiol functionalized mesoporous silica nanoparticles packed on cartridges by micro column fast micro solid-phase extraction were investigated [28]. Modification of graphene for speciation of chromium in wastewater samples by suspension solid-phase microextraction procedure was studied [29]. Magnetic nanomaterials have attracted significant interest in the past few decades because of their unique properties such as superparamagnetism. Among them, iron-based magnetic nanomaterials, which exhibit special physical and chemical properties, have been successfully adapted to many applications in a wide range of fields, including catalysis, biotechnology, biomedicine, magnetic resonance imaging, data storage, biosensors, and removal of environmental pollutants, among others [30-35]. Ezzatzadeh et al [36] were investigated synthesis of magnetic iron-oxide nanofiber composite using electrospinning: an absorbent for removal of nitrate from aqueous solution. The functionality of designing filter against affecting parameters along with the relation of these parameters with each other on the removal efficiency of nitrate was evaluated. It is concluded from the results that the height of the nano filter and the amount of magnetic nanoparticles has the most significant effect on the nitrate removal from water among all other factors. Rezaei kalantary et al [37] were studied Nitrate adsorption by synthetic activated carbon magnetic nanoparticles: kinetics, isotherms and thermodynamic studies. The results show that the activated carbon-Fe_3O_4 MNP (AC-Fe_3O_4 MNP) could be applied as a proper adsorbent for the removal of nitrate from aqueous solutions due to the advantages of high efficiency, rapid separation, and multiple usages. RSM, as a practical and economical method for process optimization, consists of three distinct steps. In an efficient RSM optimization, the first step deals with the proper experimental design for successful evaluation of the model parameters. The second step involves fitting a polynomial model to the experimental data, and investigating the suitability of the obtained model through statistical tests [38-41].

In this study, due to the importance of the

subject of economically, environmentally, and possibility of production in high scale and rapid separation, magnetic $CoFe_2O_4$ particles Were obtained by precipitation method and clinoptilolite was modified by $CoFe_2O_4$ nanoparticles and characterized. The adsorption of nitrate by clinoptilolite and clinoptilolite/ $CoFe_2O_4$ was studied further. Finally, the effect of parameters such as temperature, time, and adsorbent mass was optimized by the RSM through the BBD method.

MATERIALS

Cobalt nitrate ($Co(NO_3).6H2O$)CAS Number:10026-22-9,Iron(III) Nitrate nonahydrate (Fe(NO3)3.9H2O)CAS Number:7782-61-8,Sodium hydroxide (NaOH)CAS Number:1310-73-2,and Potassium nitrate(KNO3)CAS Number: 7757-79-1were purchased Merck Co.Clinoptilolite sample used in this work was collected from the mines of Semnan (Iran). Clinoptilolite was washed with distilled water, dried at 200°C.

Instruments

XRD patterns which were obtained with a Philips PW1800 differactometer (CuKα radiation, λ = 0.154 nm). FTIR transmission spectra of the samples were recorded by Thermo Nicolet spectrometer (Nexus 870, USA) with a resolution of 4 cm^{-1} in the range 4000-400 cm^{-1}. The morphology and sizes of the nanoparticles were analyzed by SEM (Sigma, Oxford Instrument, UK) and Philips E208 transmission electron microscope (TEM). Coercivity and saturation magnetization of clinoptilulite/$CoFe_2O_4$ were measured using a vibrating sample magnetometer (Meghnatis Daghigh kavir Co., Iran). Surface area, mean diameter of the cavities and the total volume of the clinoptilolite and clinoptilolite/$CoFe_2O_4$were investigated BET/BJH (BELSORP MINI II).

METHODS

Preparation of magnetic clinoptilolite /$CoFe_2O_4$

Magnetic $CoFe_2O_4$ particles were obtained by precipitation method. Specifically, 2.91 g of cobalt nitrate and 8.08 g of iron nitrate were added to 150 mL of distilled water and stirred for 30 minutes. Then, 4 g NaOH was added to the solution and was then heated in a water bath at 90 °C for 2 h.After cooling, the obtained black precipitates ($CoFe_2O_4$) were thoroughly rinsed with deionized water. The composites were prepared by mixing the 4 g clinoptilolite into water-bearing $CoFe_2O_4$and evenly dispersed through ultrasound. By a simple magnetic procedure, the obtained composites were separatedfrom water and dried in an oven at 90 °C**[42].**

Investigation of nitrate adsorption on clinoptilolite and clinoptilolite/$CoFe_2O_4$

Initially, solutions with a 100 ml volume and 100, 300, 400, 500, 700, 800 and 1200 ppm concentrations of nitrate were prepared. Then, 0.2 g clinoptilolite or magnetic clinoptilolite/$CoFe_2O_4$, was poured into nitrate solutions. The samples were stirred at 25°C for 48 hours. After a period of time, the samples were centrifuged at 12,000 rpm for 20 minutes and adsorption of samples was read by a spectrophotometer.

The data obtained in the batch studies was used to calculate the adsorption efficiency of nitrate by using the following relationship:

$$\text{Adsorption efficiency \%} = \frac{(C_i - C_e)}{C_i} * 100\% \quad (1)$$

Where C_i and C_e are concentrations of nitrate in the initial and final solutions, respectively.

Also, the q_e was calculated following equation [43,44]:

$$q_e = \frac{V(C_o - C_e)}{W} \quad (2)$$

Where q_e is the equilibrium adsorption capacity (mg/g), C_0 is the initial concentration of metal in solution (mg/L), C_e is the concentration of metal in solution (mg/L), V is the amount of solvent (L) and W adsorbent weight (g).

Experimental Design

At first, 100 ml nitrate solutions at 100 ppm concentration were prepared. Then, 0.1, 0.2 and 0.3 g of clinoptilolite/$CoFe_2O_4$, were poured into nitrate solutions. The samples were stirred at 25, 52.5 and 80 °C for 12, 30 and 48 hours. After a period of time, the samples were centrifuged at 12,000 rpm for 20 minutes and adsorption of samples was read by a spectrophotometer.

Response surface methodology

The response surface methodology is a powerful statistical modeling tool that runs on based on the smallest number of empirical experiments according to the design of the test. Currently, RSM is widely used to optimize the adsorption process variables [44]. RSM is based on a non-linear multi-variable model that consists of a test design

Table 1. Independent variables and their levels in the experimental

Independent variables	Coded symbols	Levels
Temperature (°C)	X_1	25, 52.5, 80
Time (h)	X_2	12, 30, 48
Adsorbent (g)	X_3	0.1, 0.2, 0.3

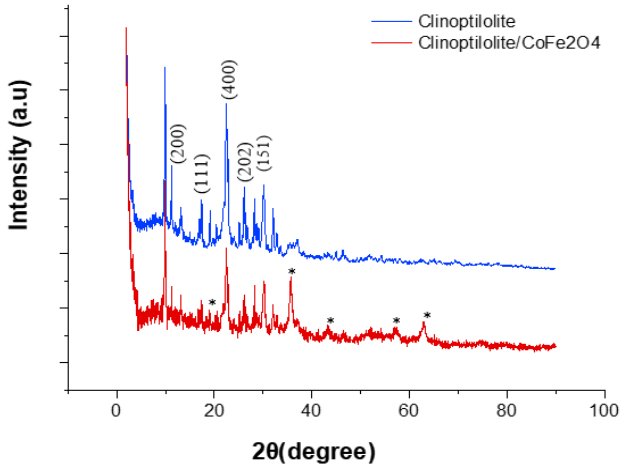

Fig. 1. XRD patterns of the a) clinoptilolite, b) clinoptilolite/$CoFe_2O_4$.

to provide sufficient and reliable response values, followed by a mathematical model that has the best fit with the experimental design information, and the optimal value of the independent variables, which determines the highest or lowest response. RSM has varieties and can be used in different ways. One of its types is the Box-Behnken method. This method can estimate the value of parameters in a quadratic model, construct the required design and compute the magnitude of non-matching parameter. Comparison between BBD designs and other responsiveness designs (central composite design or full factorial design) shows that BBD is far more efficient than both central composite design and full factorial design. This cubic design is described by a set of hypothetical points, at the midpoint of each side of a multidimensional cube and the repetition of the center point. This scheme allows the answers to be modeled by fitting a second-order polynomial, which can be expressed as the following equation:

$$Y = \beta_0 + \sum_{j=1}^{k} \beta_j X_j + \sum_{j=1}^{k} \beta_j X_j^2 + \sum_{i} \sum_{<j=2}^{k} \beta_j X_i X_j + e_i \quad (3)$$

Where Y is the predicted response (predicted adsorption capacity); $X_i$and X_j are the independent variables in coded levels; β_0 is the intercept. β_i, β_{jj}, β_{ij} are the linear, squared and interaction effect coefficients respectively. k is the number of factors (independent variables) and e_i is the model error.

The number of experiments is obtained from the following equation:

$$N=2K(K-1)+C_0 \quad (4)$$

Where K is the number of variables, C_0 is the number of central points. In this study, K and C_0 were set to 3, in which case 15 tests should be done.

In this study, the experiments planned with 3 factors of temperature, time and mass of adsorbent are shown in the Table 1.

RESULT AND DISCUSSION

X-ray diffraction (XRD) is one of the unique equipment for analyzing and characterizing crystals in the laboratory. XRD is an effective method to investigate the existence of $CoFe_2O_4$ in composites. XRD patterns of the clinoptilolite and clinoptilolite/$CoFe_2O_4$ are shown in Fig. 1. The pattern of clinoptilolite (standard card JCPDS 01-083-1261) is shown in Fig. 1. The pattern of pure $CoFe_2O_4$(standard JCPDS card 22-1086)exhibited sharp peaks at 2θ angles of 18.3, 30.1, 35.4, 43.1,

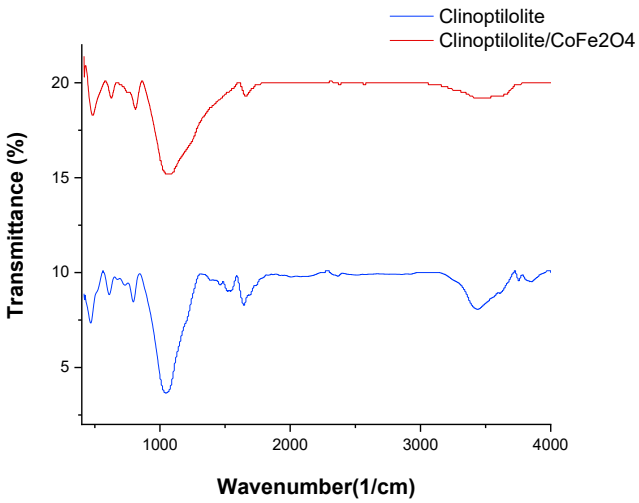

Fig. 2. FT-IR spectra of the a) clinoptilolite, b) clinoptilolite/$CoFe_2O_4$.

57.0 and 62.6°indicating that the cubic spinel phase $CoFe_2O_4$ was well obtained.

According to Equation (5), the average particle size was estimated according to Debye–Scherrer:

$$B=\frac{K\lambda}{Lcos\theta} \quad (5)$$

B crystallite size, K constant equal to 0.89, λ the cathode wavelength (nm), L FWHM (rad) and θ angle corresponding to the desired peak. The average particle size calculated from the Debye–Scherrer for clinoptilolite and clinoptilolite/$CoFe_2O_4$ were about 31 nm and 42 nm, respectively. The interaction of infrared radiation with a sample changes the vibrational energy of the bond in its molecules and is a good way to identify the functional groups and molecular structure. The condition for the absorption of infrared energy by the molecule is that the dipole moment changes during vibration. The FT-IR spectra of the clinoptilolite and clinoptilolite/$CoFe_2O_4$are presented in Fig. 2. Zeolite is a mineral that consists mainly of aluminous silicates and contains a percentage of the elements Mn Ca, Fe, Mg, Na. In the FTIR spectrum, clinoptilolite has 2 main lines. The Si-O-Si and Si-O-Al phase in the 1040 cm^{-1} area, which is related to Si-O-Si asymmetric tensile vibration, overlaps with Al-O-Al tensile vibrations. According to the geometrical configuration of the oxygen nearest neighbors, the metal ions are usually situated in two different sublattices in ferrites, designated astetrahedral and octahedral sites. The vibration spectra of $CoFe_2O_4$at the high-frequency band 609cm^{-1} and the low-frequency band 466 $cm^{-1}$are attributed to the intrinsic vibration of the tetrahedral sites and the octahedral sites, respectively.

Scanning electron microscopy (SEM) is one of the most suitable tools analyzing the morphology of nanostructures and identifying chemical compounds using Energy Dispersive X-ray Analysis. To investigate the morphology and structure of the prepared clinoptilolite and clinoptilolite/$CoFe_2O_4$, scanning electron microscope (SEM) micrographs are shown in Fig. 3.As shown in Fig. 3a, the surface of untreated clinoptilolite is clean, almost uniform and containing interconnected pores.Fig.3b illustrates the surface after modification procedure .Based on the obtained results, cobalt ferrite has been loaded onto clinoptilolite. The average particle size is comparable with the Debye Scherrer calculated crystallite size.

The transmission electron microscope (TEM), the first type of electron microscope, is a special tool for determining the structure and morphology of materials. Fig. 4 shows the TEM images of clinoptilolite before and after magnetic modification. It can be seen from Fig. 4a that the raw clinoptilolite appears in an irregular morphology, but its surface and boundary is clear. As shown in Fig. 4b, $CoFe_2O_4$nanoparticles cover evenly on the surface of clinoptilolite, which is important for the composites to enhance the magnetic separate recovery rate.

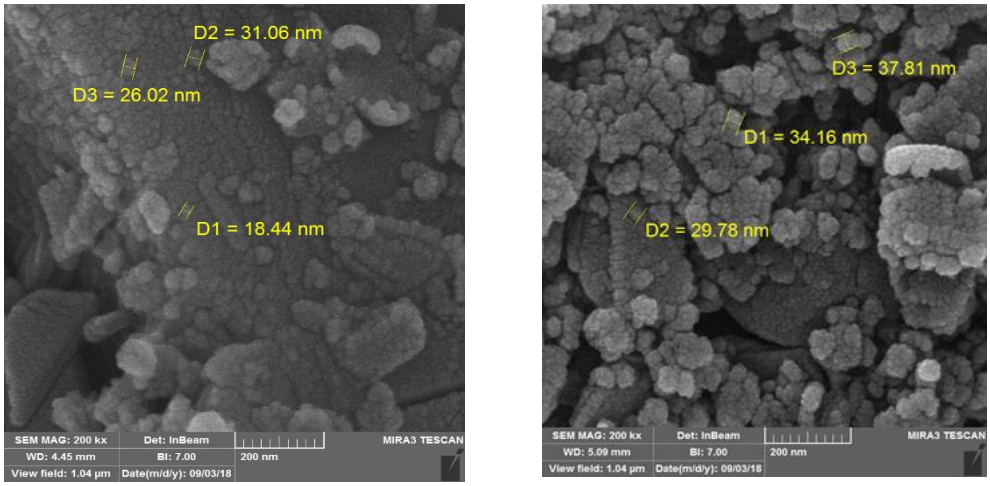

(a) (b)

Fig. 3. SEM images of the a) clinoptilolite(200nm),b) clinoptilolite/$CoFe_2O_4$(200nm)

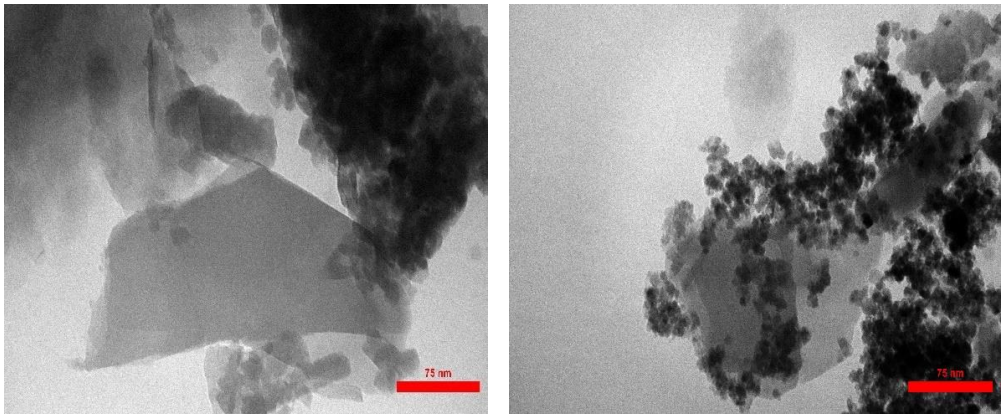

(a) (b)

Fig. 4. TEM images of the a) clinoptilolite, b) clinoptilolite/$CoFe_2O_4$.

Brunauer-Emmett-Teller (BET) surface area analysis and Barrett-Joyner-Halenda (BJH) pore size and volume analysis. BET analysis provides specific surface area evaluation of materials by nitrogen multilayer adsorption measured as a function of relative pressure. Using the BET method, the surface area of clinoptilolite and clinoptilolite /$CoFe_2O_4$was determined. Also, through the BJH method, the mean diameter of the cavities and the total volume of the cavities were determined. The absorption/desorption nitrogen isotherms offer porous structure, properties for clinoptilolite and clinoptilolite/$CoFe_2O_4$, with the results being presented in Fig. 5 and Table 2. Based on the results, the surface area increased from 18.42 to 25.95 m^2 $g^{-1}$by modification of clinoptilolite surface.Also, through the surface modification, the mean pore diameter was decreased.

Vibrating sample magnetometry (VSM) belongs to the direct class of magnetic measuring techniques, where the macroscopic magnetization of the sample is sensed. Paramagnetic materials

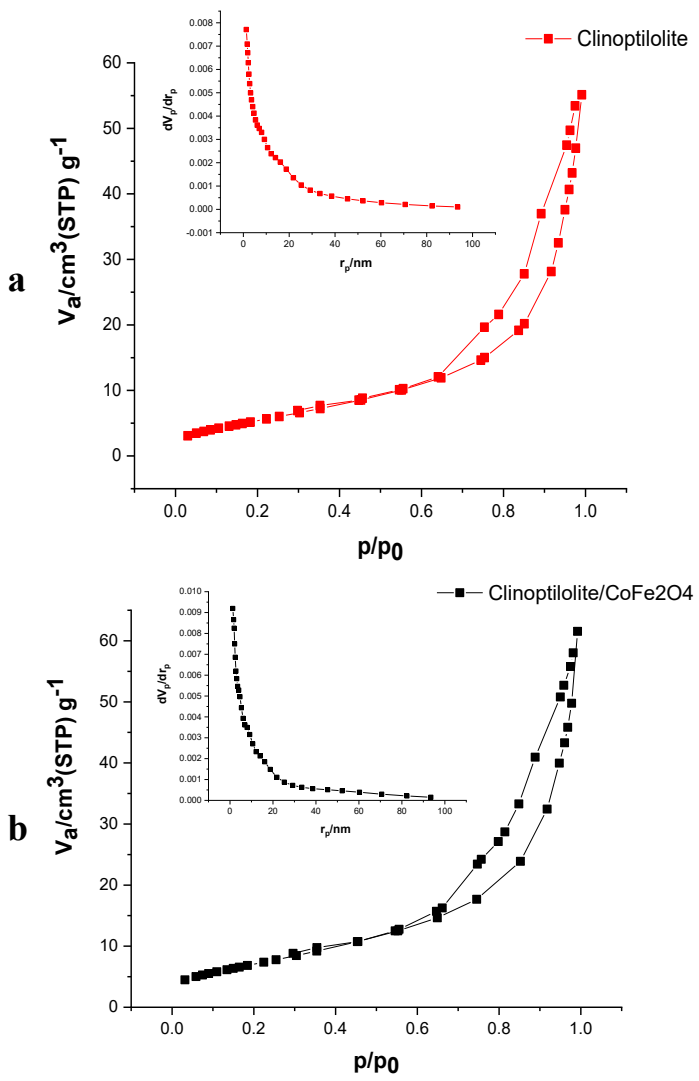

Fig. 5. Nitrogen adsorption/desorption isotherms a) clinoptilolite, b) clinoptilolite/$CoFe_2O_4$.

Table 2. Results of BET / BJH analysis of adsorbents.

Adsorbent	Vm ($cm^3(STP)g^{-1}$)	$a_{s,BET}$ (m^2g^{-1})	Mean pore diameter (nm)	Total pore volume ($cm^3\ g^{-1}$)
Clinoptilolite	4.2	18.42	16.65	0.08
Clinoptilolite/$CoFe_2O_4$	5.96	25.95	14.25	0.09

are substances which when placed in a magnetic field are feebly magnetized in the direction of the magnetizing field. A material is super paramagnetic if it is made of very small single-domain non-interacting magnetic grains dispersed in some non-magnetic medium. Magnetization curves for the clinoptilolite/$CoFe_2O_4$are shown in Fig. 6.Meanwhile, due to the magnetization curve of the magnetic clinoptilolite/$CoFe_2O_4$magnetic nanocomposite, it can be concluded that the hysteresis ring, a waste and a residual dampening field are not significant in the curve of this nanocomposite as these materials do not require large magnetic fields for magnetization and do

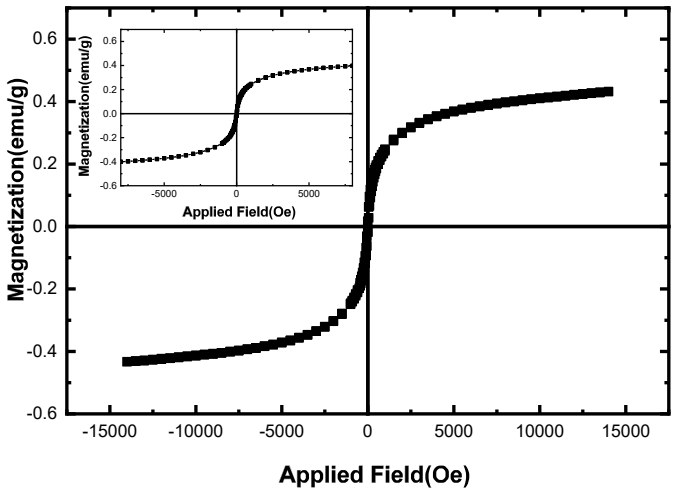

Fig. 6. Magnetization curves for the clinoptilolite/$CoFe_2O_4$.

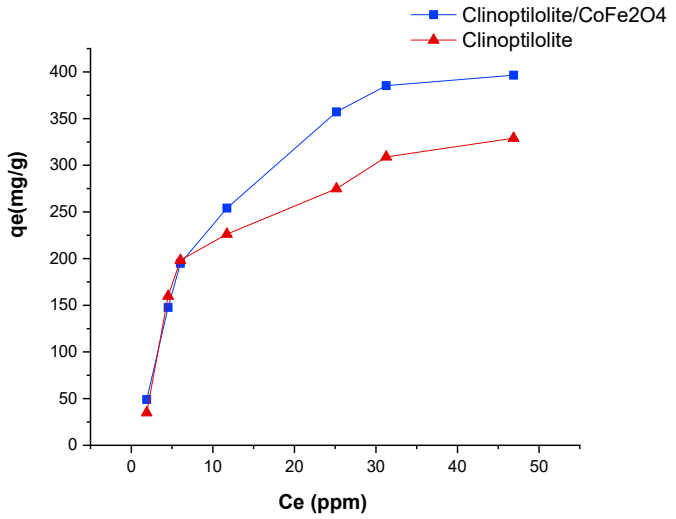

Fig. 7. Adsorption capacity by clinoptilolite and clinoptilolite/$CoFe_2O_4$.

not tend to stay magnetic; as such they are in the category of materials with magnetic properties. These particles exhibit super paramagnetic properties. Super paramagnetic is a form of magnetism which appears in small ferromagnetic or ferrimagnetic nanoparticles. This adsorbent has saturation magnetization 0.97 emu/g.

Magnetic composites adsorb pollutants from the aqueous solution and then exit the environment by a simple magnetic process. Nitrate adsorption capacity was evaluated by clinoptilolite and clinoptilolite/$CoFe_2O_4$.Based on the results, it can be concluded that the adsorption capacity of the modified clinoptilolite with magnetic nanoparticles had a higher adsorption capacity than the unmodified clinoptilolite which can be attributed to its higher surface areaand polarity in comparisonwith the unmodified zeolite. In addition magnetic property caused to easy separation of pollutants from water. The results are shown in Fig. 7.

The total number of experiments was 15 runs, which was designed as a BBD method for adsorption of nitrate on clinoptilolite/$CoFe_2O_4$(Table 3).

Fig. 8displays the assumption of the normalization of data where the data are almost normal and the results show how the residues follow a normal distribution. This indicates a very

Table 3. The BBD for the three independent variables.

RunOrder	Temperature (^{0}C)	Time (h)	Adsorbent (g)	Adsorption(%)
1	25	30	0.1	43.65
2	25	30	0.3	67.51
3	25	12	0.2	41.92
4	80	12	0.2	60.32
5	80	30	0.1	70.96
6	52.5	12	0.1	40.03
7	80	30	0.3	84.96
8	25	48	0.2	74.29
9	52.5	48	0.3	99.32
10	80	48	0.2	71.32
11	52.5	12	0.3	65.04
12	52.5	30	0.2	88.56
13	52.5	30	0.2	88.44
14	52.5	30	0.2	88.49
15	52.5	48	0.1	75.25

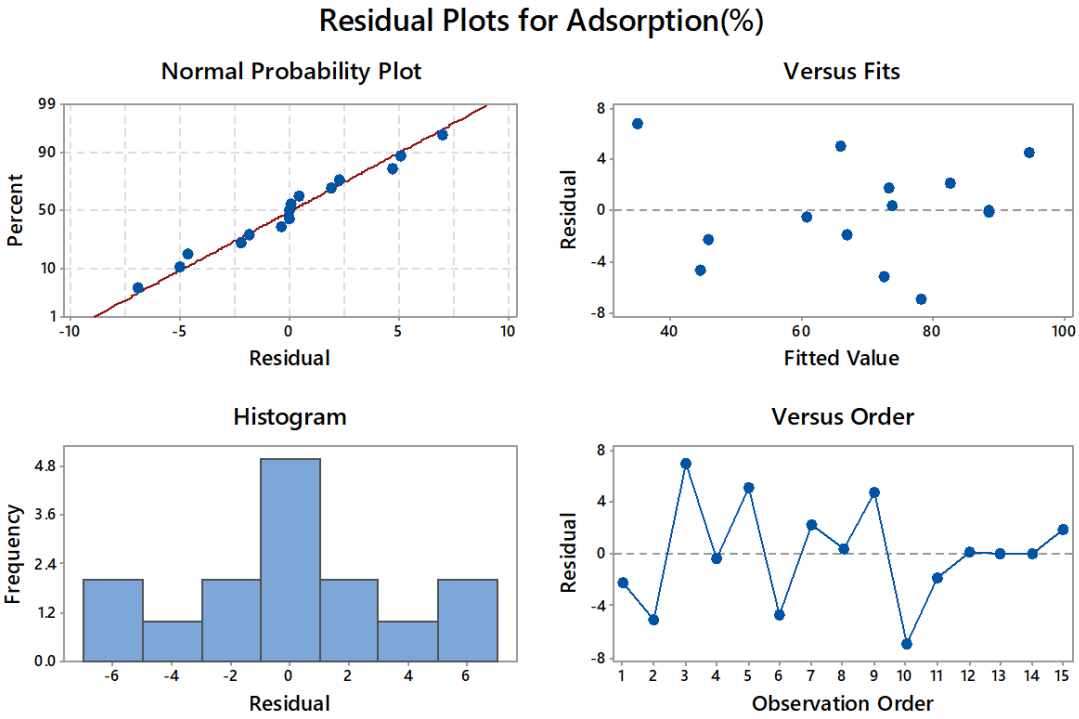

Fig. 8. Residual Plots to study of adsorption nitrate.

Table 4. ANOVA for analysis of variance and adequacy of the quadratic model for nitrate adsorption

Source	DF	Adj SS	Adj MS	F-Value	P-Value
Model	9	4448.63	494.29	11.85	0.007
Linear	3	2990.13	996.71	23.89	0.002
Temperature (^{0}C)	1	452.85	452.85	10.85	0.022
Time (h)	1	1592.45	1592.45	38.17	0.002
Adsorbent (g)	1	944.82	944.82	22.64	0.005
Square	3	1319.8	439.93	10.54	0.013
Temperature (^{0}C)*Temperature (^{0}C)	1	812.82	812.82	19.48	0.007
Time (h)*Time (h)	1	505.19	505.19	12.11	0.018
Adsorbent (g)*Adsorbent (g)	1	175.26	175.26	4.2	0.096
2-Way Interaction	3	138.7	46.23	1.11	0.428
Temperature (^{0}C)*Time (h)	1	114.17	114.17	2.74	0.159
Temperature (^{0}C)*Adsorbent (g)	1	24.3	24.3	0.58	0.48
Time (h)*Adsorbent (g)	1	0.22	0.22	0.01	0.945
Error	5	208.62	41.72		
Lack-of-Fit	3	208.61	69.54	19138.92	0.05
Pure Error	2	0.01	0		
Total	14	4657.25			

Adsorption (%) = -112.4 + 2.837 Temperature (^{0}C) + 3.543 Time (h) + 435 Adsorbent (g) - 0.01962 Temperature (^{0}C)*Temperature (^{0}C) - 0.0361 Time (h)*Time (h) - 689 Adsorbent (g)*Adsorbent (g) - 0.01079 Temperature (^{0}C)*Time (h) - 0.90 Temperature (^{0}C)*Adsorbent (g) - 0.13 Time (h)*Adsorbent (g)

good correlation between the results obtained by the experimental method and the values predicted by the statistical method.

Regarding the ANOVA, the R-Squared and Adj R-Squared values are 0.952 and 0.8746, respectively, which are approximately equal to one and represent the correctness of the model.

Among the factors, time, adsorbent mass and temperature influenced the adsorption process respectively. The results of analysis of variance for the quadratic response level model to the experimental data are shown in Table 4.In this study, the factors of time, adsorbent mass, and temperature were affected.

Effect of time, mass of adsorbent, and temperature

In general, one of the most important parameters affecting the adsorption process is the time effect. The results of the experiments indicated that the nitrate removal efficiency, increased with time because as the contact time increased, the nitrate solution had a longer opportunity for adsorption. So in this study, the maximum removal was observed 40 h after which the removal efficiency reached equilibrium. The reaction temperature plays a decisive role in the adsorption process. The results showed that with temperature rise from 25 to 50 °C, the efficiency increased and then decreased with elevation of temperature from 50 to 80°C. Also, the results showed that as the adsorbent dose increased, so did the removal efficiency due to the increase in active sites for adsorption.Fig.9 shows the effect of time, adsorbent mass, and temperature in the two-dimensional and three-dimensional forms.

Determining optimal conditions

According to experimental design studies, the optimal point conditions were obtained. Under optimum conditions, the best point for achieving the highest adsorption efficiency was 55 ° C, 40.36 h, and 0.27 g, 97.03%. The results are displayed in Fig. 10.

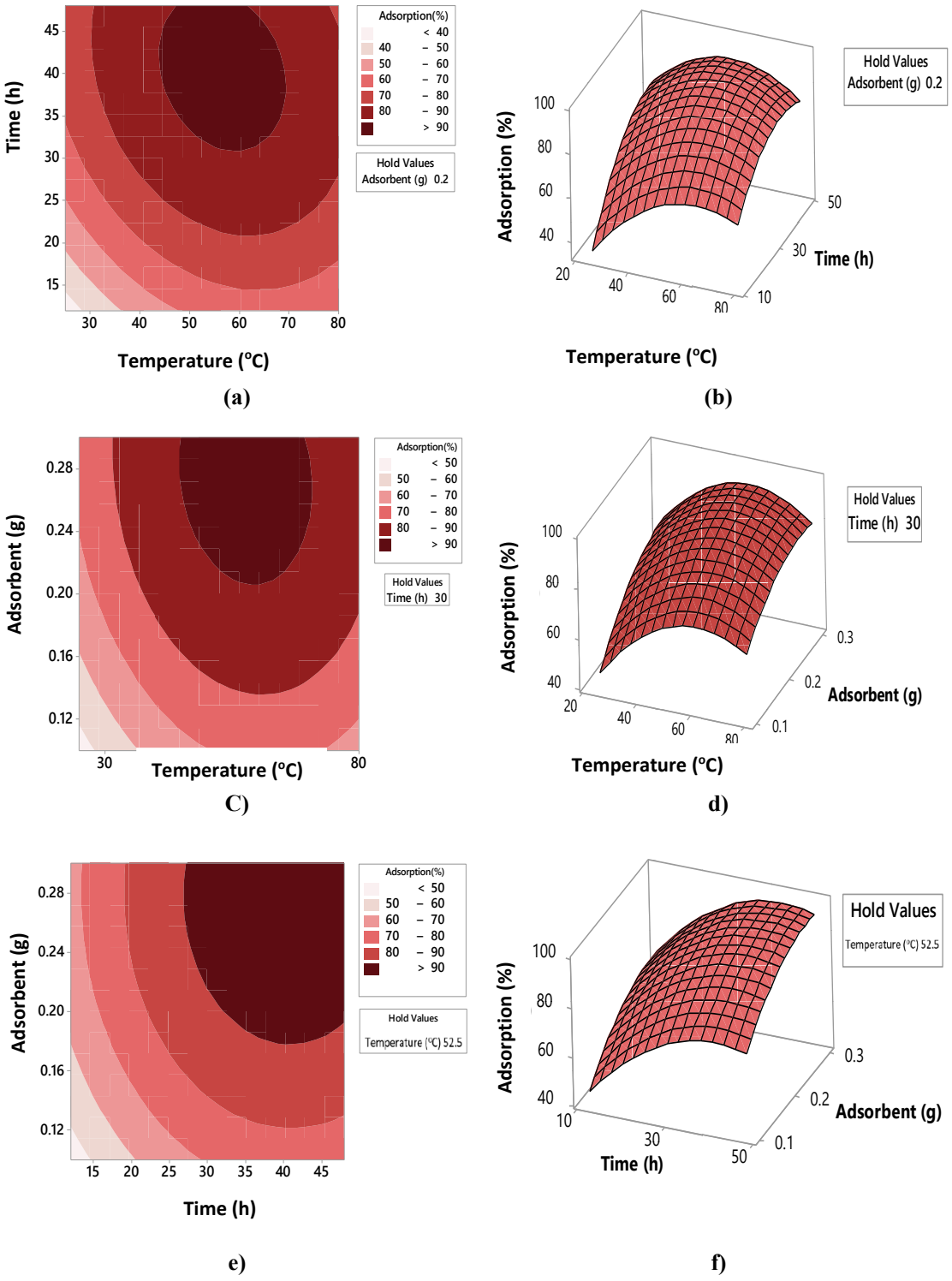

Fig. 9. Contour plots adsorption versus a) time and temperature, c) adsorbent and temperature, e) adsorbent and time and 3D plots adsorption versus b) time and temperature, d) adsorbent and temperature, f) adsorbent and time.

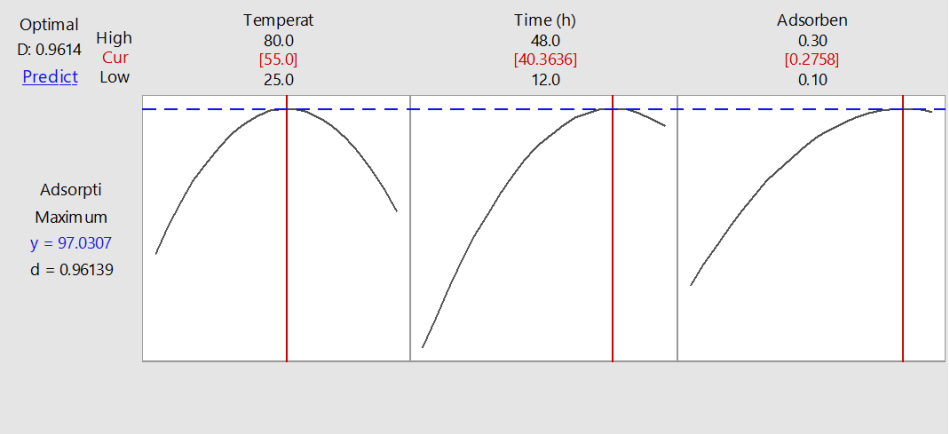

Fig. 10. Graphs the optimum conditions for adsorption of nitrate using clinoptilolite /$CoFe_2O_4$.

Table 5. shows the performance of other adsorbents with clinoptilolite /$CoFe_2O_4$ adsorbent. Based on the results the magnetic clinoptilolite /$CoFe_2O_4$ is low cost and high performance.

Adsorbent	Adsorbate	Adsorption efficiency	Reference
carbon-silicon nano composites	Nitrate	45.35%	[45]
Anionic rice husk	Nitrate	94.3%	[46]
γ-Fe_2O_3@hydroxyapatite nanoparticles	Nitrate	93-99%	[47]
Clinoptilolite /$CoFe_2O_4$	Nitrate	97.03%	This work

CONCLUSION

In this study, clinoptilolite and clinoptilulite/$CoFe_2O_4$characterized by XRD, IR, SEM, TEM,BET/BJH,and VSM techniques. According to the importance of the subject frugality, environmental requirements, and the possibility of production on a high scale clinoptilulite/CoFe2O4, magnetic cobalt ferrite particles were synthesized by precipitation method combined with clinoptilolite. .The pattern of pure $CoFe_2O_4$(standard JCPDS card 22-1086) indicating that the cubic spinel phase $CoFe_2O_4$ obtained. Nitrate adsorption capacity was evaluated by clinoptilolite and clinoptilolite/$CoFe_2O_4$. These results indicated that the CoFe2O4 present on the surface of clinoptilolite enhances the adsorption performance. The effect of different variables on the nitrate removal process, including temperature, time, and mass of adsorbent, was optimized using the RSM with the BBD method. Among the factors, time, adsorbent mass, and temperature were affected. Under optimum application conditions, the best point for achieving the highest adsorption efficiency (97.03%) was 55 °C, 40.36 h, and 0.27 g mass of adsorbent.

CONFLICT OF INTEREST

The authors declare that there is no conflict of interests regarding the publication of this manuscript.

REFERENCES

1. N. Bombuwal Dewage, A. S. Liyanage, Ch. U. Pittman Jr., D. Mohan, T. Mlsn. Bioresour. Technol., 263, 258–265 (2018).
2. P. Li, K. Lin, Zh. Fang, K. Wang. J. Clean. Prod., 151, 21-33 (2017).
3. Giorgio Vilardi. Luca Di Palma. Bull. Environ. Contam. Toxicol., 98(3), 359-365 (2017).
4. J. Wang,L. Chu. Biotechnol. Adv., 34, 1103-1112 (2016).
5. Y. Zeng,H. Walker,Q. Zhu. J. Hazard. Mater.,324, 605-616 (2017).
6. A. Teimouri,Sh. GhanavatiNasab,N. Vahdatpoor,S. Habibollahi,H. Salavati,A. NajafiChermahini,Int. J. Biol. Macromol., 93, 254-266 (2016).
7.I. Pantelaki, D. Voutsa,Science of the Total Environment., 613–614, 389-397 (2018).
8.M.Sillanpää,M.ChakerNcibi,A. Matilainen,M. Vepsäläinen,j.Chemosphere.,190, 54-71 (2018).
9. G. Sharma, D. Pathania, M. Naushad, 21, 1045-1055 (2015).
10.S.Gabarróna, W.Gernjakac, F.Valerob, A.Barcelób, M.Petrovicac,I.Rodríguez-Rodaa,J. Hazard. Mater.,309, 192-201 (2016).

11. J. Radjenovic, D. L. Sedlak, Environ. Sci. Technol.,4919, 11292-11302 (2015).
12. K. Y. Hor,J. Mun, Ch. Chee,M. N. Chong,B. Jin,Ch. Saint,P. E. Poh,R. Aryal,J. Clean. Prod., 118, 197-209 (2016).
13. M. Moradi,R. Karimzadeh,E. Sadat Moosavi,Fuel.,217, 467-477 (2018).
14. F. Eshraghi, A. Nezamzadeh-Ejhieh,Environ Sci Pollut Res Int., 25, 14043-14056 (2018).
15. N. Kashi, N. Elmi Fard, R. Fazaeli,Russ. J. Appl. Chem., 90, 977-1992 (2017).
16. T. Amiri-Yazani, R. Zare-Dorabei, M. Rabbani, A. Mollahosseini,Microchem. J., 146, 498–508 (2019).
17. M. Yuan, T. Xie, G. Yan, Q. Chen, L. Wang,J.powtec.,332, 234-241 (2018).
18. Zh.Wang, K.Tan, J.Cai, Sh.Hou, Y.Wang,P.Jiang,M. Liang,Colloids and Surfaces A: Physicochem. Eng. Aspects., 561,388-394 (2019).
19. M. Majlesi Nasr, K. Rahmani, H. Rahmani, M. Yousefi, A. Rahmani,J. Health.8, 280-288 (2017).
20. A. Ghamkhari, A.Rahdar, S. Rahdar, M. A. B. H. Susan, Nano-Structures & Nano-Objects., 19, 100371 (2019).
21. S.M. Taimoory, A. Rahdar, M. Aliahmad, F. Sadeghfar, M.R. Hajinezhad, M. Jahantigh, J.F. Trant, J. Mol. Liq., 265, 96-104 (2018).
22. T.M. Hakami, A.M. Davarpanah, A. Rahdar, S. D. Barrett, J. Mol. Struct, 1165., 344-348 (2018).
23. Sh. Ahmadi, A. Rahdarb, S. Rahdara, Ch. Adaobi Igwegbe. Desalin. Water. Treat., 152:401-410 (2019).
24. A. Rahdar, M. Aliahmad, M.R. Hajinezhad, M. Samani,J. Mol. Struct., 1173, 166-172 (2018).
25. A.M. Khan, F. Shafiq, S.A. Khan, S. Ali, B. Ismail, A.S. Hakeem, A. Rahdar, M.F. Nazar, M. Sayed, M.A.R. Khan,J. Mol. Liq., 274, 673-680 (2019).
26. E. Zolfonoun, Anal. Meth. Environ. Chem. J., 1(01), 5-10 (2018)
27. B.Fahimirad,A. Asghari, Anal. Meth. Environ. Chem., 1(01), 47-56 (2018).
28. M. Gou, B.B. Yarahmadi, Anal. Meth. Environ. Chem., J, 2(03), 39-50 (2019).
29. A. Ghozatloo, Anal. Meth. Environ. Chem. J., 2(03), 51-66 (2019).
30. K. Zhu, Y. Ju, J. Xu, Z. Yang, S. Gao, Y. Hou, Acc. Chem. Res.,51(2), 404-413 (2018).
31. Q. Zhou, J. Li, M. Wang, D. Zhao,CRIT. REV. ENV. SCI. TEC., 46(8), 783-826 (2016).
32. A. Houshangi, S. Jamehbozorgi, M. Yousefi. R. Ghiasi, J. Chin. Chem, Soc.,67(2),288-297,(2020).
33. A. S.Shariatdoost, M. Yousefi , p.derakhshi, A. Safekordi, k. larijani, J. Nanoanalysis., 5(1),1-6(2018).
34. F. Tavakolinia, M. Yousefi, S.S.S. Afghahi, S. Baghshahi, S. Samadi, Process. Appl. Ceram., 12 (3), 248-256(2018).
35. T. Navaei Diva, K. Zare, F. Taleshi, M. Yousefi, J .Nanostruct. Chem., 7, 273-281(2017).
36. E. Ezzatzadeh, M.M. Langroudi, F.J. Sheshdeh, J. Appl. Chem., 11(4), 46-59 (2017).
37. R. Rezaei Kalantary, E. Dehghanifard, A. Mohseni-Bandpi, L. Rezaei, A. Esrafili, B.Kakavandi, A. Azari, Desalin. Water. Treat., 57(35), 16445-16455 (2016).
38. Z.R. Lazic, WILEY-VCHVerlagGmbH and Co. KGaA, Germany., (2004)
39.R.L. Mason, R.F. Gunst,J.L. Hess, 2nd ed. John Wiley and Sons, USA (2003).
40. D.C. Montgomery, Design Analysis of Experiments, 4th ed. John Wiley and Sons,
USA (1996).
41. B. Pouladi, M. A. Fanaei, Gh. Baghmisheh,J. Clean. Prod.,209, 965-977 (2019).
42. Y. Huang,W. Wang, Q. Feng, F. Dong, J. Saud. Chem. Soc.,21(1), 58-66 (2017).
43. N. Elmi Fard, R. Fazaeli, R. Ghiasi, Chem. Eng. Technol.,39, 1, 149-157 (2016).
44. R. Saadi, Z. Saadi, R. Fazaeli, N. Elmi Fard,Korean. J. Chem., Eng. 32, 787-799 (2015).
45. M.Muthu, D. Ramachandran, N. Hasan, M. Jeevanandam, J. Gopal, S. Chun. Mater. Chem. Physic., 189, 12-21 (2017).
46.R. Katal, M.S. Baei, H.T. Rahmati, H. Esfandian,J. Ind. Eng. Chem., 18(1), 295-302 (2012).
47. E. Ghasemi, M. Sillanpää,J. separa. sci, 38(1).,164-169 (2015).